HHS Public Access

Author manuscript

Immunobiology. Author manuscript; available in PMC 2021 January 01.

Published in final edited form as:

Immunobiology. 2020 January ; 225(1): 151867. doi:10.1016/j.imbio.2019.11.002.

Neutrophil extracellular traps impair fungal clearance in a mouse model of invasive pulmonary aspergillosis

Astrid Alflen[a], **Pamela Aranda Lopez**[a], **Ann-Kathrin Hartmann**[b], **Joachim Maxeiner**[c], **Markus Bosmann**[d,e], **Arjun Sharma**[d,e], **Johannes Platten**[d], **Frederic Ries**[a], **Hendrik Beckert**[f], **Wolfram Ruf**[d], **Markus P. Radsak**[a,*]

[a]Department of Internal Medicine III, University Medical Center of the Johannes Gutenberg University, Mainz, Germany

[b]Institute for Immunology, University Medical Center of the Johannes Gutenberg University, Mainz, Germany

[c]Asthma Core Facility, University Medical Center of the Johannes Gutenberg University, Mainz, Germany

[d]Center for Thrombosis and Hemostasis, University Medical Center of the Johannes Gutenberg University, Mainz, Germany

[e]Pulmonary Center, Department of Medicine, Boston University School of Medicine, Boston, USA

[f]Department of Pulmonary Medicine, University Medical Center Essen – Ruhrlandklinik, Essen, Germany

Abstract

Neutrophil extracellular traps (NETs) are formed by polymorphonuclear neutrophils (PMN) and contribute to the innate host defense by binding and killing bacterial and fungal pathogens. Because NET formation depends on histone hypercitrullination by peptidylarginine deiminase 4 (PAD4), we used PAD4 gene deficient (*Pad4*$^{-/-}$) mice in a mouse model of invasive pulmonary aspergillosis (IPA) to address the contribution of NETs to the innate host defense *in vivo*. After the induction (24 h) of IPA by *i.t.* infection with *Aspergillus fumigatus* conidia, *Pad4*$^{-/-}$ mice revealed lower fungal burden in the lungs, accompanied by less acute lung injury, TNFα and citH3 compared to wildtype controls. These findings suggest that release of NETs contributes to tissue damage and limits control of fungal outgrowth. Thus inhibition of NETosis might be a useful strategy to maintain neutrophil function and avoid lung damage in patients suffering from IPA, especially in those suffering from preexisting pulmonary disease.

*Corresponding author at: Department of Internal Medicine III, University Medical Center of the Johannes Gutenberg University, Langenbeckstraße 1, Mainz, Rheinland-Pfalz, 55131, Germany. radsak@uni-mainz.de (M.P. Radsak).

Author contributions

AA performed experiments and wrote the manuscript. PAL, AKH, JM, AS, JP, FR and HB performed experiments. WR, MB and MPR designed the study.

Declaration of Competing Interest

The authors have no conflicts of interest to declare.

Keywords

Neutrophil extracellular traps; *Aspergillus fumigatus*; Pneumonia; Peptidylarginine deiminase 4; Neutrophils

1. Introduction

Aspergillus fumigatus (A. fumigatus) is a ubiquitous mold that is generally benign in immunocompetent individuals. However, immunocompromised patients suffering from hematologic disorders, chemotherapy-induced neutropenia or experiencing solid organ or hematopoietic stem cell transplant are at extreme risk of developing invasive aspergillosis. In this group of patients, fungal infections, including invasive pulmonary aspergillosis (IPA), are responsible for significant morbidity and mortality (Chamilos et al., 2006; Kontoyiannis et al., 2010; Pagano et al., 2010; Pappas et al., 2010). Due to its constant exposure to airborne *A. fumigatus* spores or conidia, the lung is a major target organ (Romani, 2004). Although various drugs are nowadays available for the treatment of this infectious complication (Stewart and Thompson, 2016), the presence and functionality of polymorphonuclear neutrophils (PMN) (Stadler et al., 2017) play a major role in overcoming the disease. Therefore replacement with granulocyte transfusion for patients with neutropenia seemed a rational approach. Demla et al. summed up, that despite conflicting data, granulocyte transfusion appears beneficial in the management of this population but selection criteria for the patients are needed, as well as caution in patients with respiratory infections (Demla et al., 2016).

In the first interaction with the host *A. fumigatus* has to overcome different barriers that protect the healthy, immunocompetent host from infections. Besides the anatomical barriers to *Aspergillus* infection, the airway epithelium plays a mayor role in combatting this germ. *A. fumigatus* is molecularly recognized by soluble as well as membrane bound receptors (*e.g.* dectin-1, toll-like receptors) leading to cellular responses. Besides the initial involvement of alveolar macrophages, PMN, eosinophils, natural killer (NK) cells, monocytes and platelets, dendritic cells mediate an adaptive immune response. Nevertheless, there is no doubt that alveolar macrophages and PMN play a major role in the first line of defense against this fungal pathogen (Margalit and Kavanagh, 2015). After PMN recognize the fungus by diverse pathogen recognition receptors, the activation of signal transduction pathways triggers a number of cytotoxic effector mechanisms in PMN, including reactive oxygen species (ROS) production by the nicotinamide adenine dinucleotide phosphate (NADPH) oxidase system, the formation of neutrophil extracellular traps (NETs), and the release of granula-derived proteases and microbicidal peptides (Kolaczkowska and Kubes, 2013).

PMN sense microbe size and selectively release NETs in response to large pathogens like *A. fumigatus* hyphae or large aggregated conidia but not in response to small single conidia (Branzk et al., 2014). Hereby phagocytosis *via* dectin-1 acts as a sensor of microbe size and prevents NET release by downregulating the translocation of neutrophil elastase (NE) to the nucleus (Branzk et al., 2014). For the formation of NET, ROS trigger the dissociation of NE

from a membrane-associated complex into the cytosol and activates its proteolytic activity in a myeloperoxidase (MPO)-dependent manner. In the cytosol, NE first binds and degrades F-actin to arrest actin dynamics and subsequently translocates to the nucleus (Metzler et al., 2014). Finally, NETs contain granule proteins and chromatin that together form extracellular fibers that bind microorganisms. Thereby they are prevented from spreading and a high local concentration of antimicrobial agents to degrade virulence factors and kill bacteria is ensured (Brinkmann et al., 2004). Although fungi are able to induce NETs, they do not seem to be involved in the PMN-mediated killing of *Aspergillus* and *Candida* spp. (Gazendam et al., 2016). However, the ability of NET-dependent fungal killing remains controversial (Gazendam et al., 2016; Urban et al., 2006).

Besides the crucial role of NET formation in host defense against microorganisms, an excess or persistence of NET release is potentially injurious to host organs and cells. The pathogenicity of NET is especially important in pulmonary diseases due to the lung architecture itself, where tissue damage and impairment in lung function is enhanced. To date, recombinant human DNase is the only treatment targeting NETs approved for a small number of pulmonary disorders (Porto and Stein, 2016).

In the present study, we evaluated the role of NETosis in the innate immune responses elicited by *A. fumigatus* in a murine model of IPA. We employed PAD4 deficient ($Pad4^{-/-}$) and wildtype mice and analyzed severity and course of infection after 24 h and after one week. Furthermore, PMN effector functions were analyzed in the absence of PAD4, in murine and human cells. Therefore, the aim of this study was to assess the impact of NET formation in fungal clearance and on organ damage.

2. Materials and methods

2.1. Mice and fungal strain

$Pad4^{-/-}$ mice were on C57BL/6 J background (Hemmers et al., 2011). All animal procedures were performed in accordance with the institutional guidelines and approved by the responsible national authority (National Investigation Office Rheinland-Pfalz, Approval ID: AZ 23 177-07/G16-1-020E1). The *A. fumigatus* strain ATCC 46645 was kindly provided by M. Gunzer (Molecular Immunology, University of Duisburg-Essen, Germany) and cultured in *Aspergillus* minimal medium (Kapp et al., 2014).

2.2. Mouse model of IPA

Mice were anesthetized and received 10^7 *A. fumigatus* conidia *i.t.* as described previously (Prüfer et al., 2014). To assess the severity of infection, mice were sacrificed 24 h after induction of IPA. For the analysis of blood and bronchoalveolar lavage fluid (BALF), blood samples were collected and lungs were flushed with 1 mL PBS. Cells in the blood and BALF were analyzed by an animal blood counter (scil animal care company). The albumin amount in the BALF was quantified by standard enzyme-linked immunosorbent assay (ELISA) (Bethyl Laboratories). For the detection of inflammatory mediators in the BALF, tumor necrosis factor TNF-α ELISA (Ready-SET-Go, eBioscience) was performed and bead-based immunoassays were used (Bio-Plex Pro mouse cytokine bead-based

immunoassay, Bio-Rad). The results of the immunoassay were quantified by the Luminex xMAP/Bio-Plex 200 System with Bio-Plex Manager Software 5.0 (Bosmann et al., 2014). IL-27p28 was analyzed by an ELISA kit (R&D Systems) according to the instructions of the manufacturer. For the measurement of citH3, cell-free samples (300 g, 5 min, 4 °C) were subjected to plates coated with anti-H3Cit (abcam #ab5103, 4 μg/ml) followed by the secondary antibody and substrate of the Cell Death Detection ELISA^{PLUS} kit, v12 (Roche/Sigma-Aldrich). Optical densities (OD, 405 nm) were measured with an Opsys MR Dynex microplate reader. To determine the *in vivo* fungal burden (Prüfer et al., 2014), lungs were homogenized mechanically and serial dilutions were plated on Sabouraud 4 % glucose agar (Carl Roth). After 24 and 48 h colony-forming units (CFU) were enumerated. Some lungs were paraffin embedded and sections were stained with hematoxylin and eosin (H&E) to assess inflammatory responses and Grocott-Gomori silver stain to visualize fungi. In order to analyze the inflammation H& E-stained tissue sections were examined in blinded fashion for peribronchial, perivascular, tissue inflammation and overall pulmonary inflammation and were scored on a scale from 0 to 4 (Reuter et al., 2014). As control for the IPA mouse model, neutropenic mice were utilized. Therefore, in some mice PMN depletion was induced by *i.p.* injection of anti-Gr-1 antibody (150 μg, clone RB6-8C5) one day before infection (Alflen et al., 2017).

2.3. Invasive lung function in mice

One week after induction of IPA, wildtype and *Pad4*$^{-/-}$ mice were administered serially increasing doses of methacholine (MCh), and airway hyperresponsiveness was measured, as previously described (Böhm et al., 2015). Afterwards, bronchoalveolar lavage was performed to yield lung-infiltrating immune cells and sections of lung tissue were stained with H&E to identify inflammatory cells as described above.

2.4. Analysis of PMN functions in vitro

2.4.1. Murine white blood cells (WBC)—Heparinized blood was incubated twice (7 min and 3 min) with ammonium-chloride-potassium (ACK) lysing buffer for the lysis of red blood cells. WBC were then resolved in the medium, incubated with indicated stimuli for 2 h at 37 °C. WBC activation was measured by flow cytometry for oxidative burst, degranulation (increase in CD11b surface expression), CD62 L shedding (decrease in CD62 L expression) as well as phagocytosis, to represent PMN effector functions.

2.4.2. Murine bone marrow PMN—PMN were enriched from the bone marrow (BM) of mice by magnetic cell sorting using biotin-labeled Ly-6 G/C specific antibodies (clone RB6-8C5) and SA-beads (Miltenyi) (Prüfer et al., 2014). PMN were incubated with indicated stimuli at 37 °C for 4 h for degranulation, shedding and phagocytosis. Oxidative burst was assessed as fluorescence kinetics over a time period of 3 h.

2.4.3. Human peripheral blood PMN—Human studies were performed after obtaining informed consent from healthy volunteer donors and were approved by the local ethics committee according to the institutional guidelines (Landesärztekammer Rheinland-Pfalz, Approval no. 837.258.17 (11092)). PMN were isolated by dextran sedimentation and Histopaque® centrifugation as described previously (Alflen et al., 2018). Some PMN were

preincubated with a PAD4 inhibitor (GSK484, Sigma-Aldrich) 10 μM for 30 min at 37 °C (Lewis et al., 2015). Cells were activated with indicated stimuli. PMN functions (oxidative burst, degranulation, CD62 L shedding, viability) were assessed as described previously (Alflen et al., 2018).

2.4.4. PMN activation and analysis—PMN were treated with zymosan 10 μg/ml, lipopolysaccharides (LPS) 1 μg/ml, *A. fumigatus* conidia 106/ml and analyzed for activation after indicated time periods. For flow cytometric analysis of degranulation and shedding, gates were set on $CD11b^{high}$, and $CD62L^{low}$ PMN, respectively. Phagocytosis was assessed by simultaneous incubation with Fluoresbrite™ Polychromatic Red 1.0 μm Microspheres (Polysciences, 5.7 × 107 particles/ml) and PE intensity was measured (Prüfer et al., 2014). Phagocytosis of *A. fumigatus* conidia was evaluated after coincubation of PMN with PE-labeled conidia (0.5×10^6/ml) at 37 °C or 4 °C as negative control, respectively. Oxidative burst activity was detected by reactive oxygen intermediates that oxidized non-fluorescent dichloro-fluorescein diacetate (DCFH-DA, Sigma-Aldrich, 8,3 nM) into green fluorescent DCF (Haselmayer et al., 2007). Kinetics were measured with a fluorescence reader (SpectraFluor 4, Tecan) and values were gained as mean fluorescence intensity (MFI) (Prüfer et al., 2014), or single measurements were performed by flow cytometry. To obtain the specific fluorescence index (SFI), an index was calculated by MFI activated PMN / MFI medium PMN. Viability was assessed using CellTiter 96® Aqueous One Solution Cell Proliferation Assay (Promega) as described previously (Alflen et al., 2018). As viability control rhGM-CSF (R&D systems) 10 ng/mL was used and cyloheximide (Sigma-Al-drich) 100 μg/ml treated samples represented dead cells.

2.5. Statistical analysis

Statistical analyses were performed using GraphPad Prism (version 5.0a for Mac OS X, GraphPad Software). For comparison between two groups a Mann-Whitney *U* test was used. Comparisons of multiple groups were performed by one-way and two-way ANOVA with Bonferroni's posttest. For all analyses, $p < 0.05$ was considered as statistically significant.

3. Results

The impact of PAD4, which is essential for hypercitrullination of histones and thereby for the formation of NET, was assessed in a murine model of IPA (Fig. 1A). PAD4 deficient *(Pad4*$^{-/-}$) and wildtype mice received *Aspergillus fumigatus* conidia *intratracheally (i.t.)* on day 0. After 24 h, the severity of the infection was assessed in final examinations by analyzing blood, bronchoalveolar lavage fluid (BALF) and lungs. Some mice were observed for one week of IPA, invasive lung function analyses were performed and the experiments were completed by the final examinations described above.

3.1. PAD4 deficiency improves fungal clearance 24 h after IPA

One day after the induction of IPA, some mice were sacrificed, lungs were homogenized, serially diluted, plated on agar, incubated and monitored for 24 h (Fig. 1B) and 48 h (Fig. 1C). *Pad4*$^{-/-}$ mice revealed lower fungal burden in the lungs compared to wildtype mice, which was assessed as colony forming units (CFU) (Fig. 1B and C). To assess if less

effective fungal clearance was caused by changes in PMN recruitment, we analyzed PMN counts. However, *Pad4*$^{-/-}$ and wildtype mice showed similar PMN recruitment in the blood (data not shown) as well as into the lung tissues (Fig. 1D). Pulmonary inflammation was analyzed in a blinded fashion and an inflammation score was assessed. Inflammation was also separately studied for perivascular, peribronchial and tissue inflammation, where no differences were seen in any of these separate studies (data not shown). We also analyzed fungal burden by visualizing *A. fumigatus via* Grocott-Gomori silver stain. While it was hard to detect *A. fumigatus* conidia in wildtype and *Pad4*$^{-/-}$ animals, neutropenic control mice suffered from massive burden of hyphae (data not shown).

Since reduced fungal burden in *Pad4*$^{-/-}$ mice as compared to wildtype mice was not associated with an altered PMN recruitment, PMN functions were investigated. As expected, *Pad4*$^{-/-}$ mice, showed significantly lower amounts of citrullinated histone H3 (citH3) in the BALF of infected animals, compared to wildtype mice (Fig. 1E). Therefore, we further investigated how the deficiency of PAD4 and thereby the lack of NET formation affects the course of IPA.

3.2. PAD4 deficiency reduces lung damage 24 h after IPA

Lower amounts of citH3 in the BALF of *Pad4*$^{-/-}$ mice (Fig. 1E) were accompanied by unaltered PMN recruitment into the lung tissue (Fig. 1D), therefore BALF was also analyzed for the abundance of these innate immune cells. Very few PMN were observed in the BALF of control mice, which received H_20 *i.t.,* but infected *Pad4*$^{-/-}$ and wildtype mice showed similar numbers of PMN in the BALF (Fig. 2A). We were not able to detect any statistically significant differences in PMN recruitment into the alveolar space between the two mouse strains (Fig. 2A). Higher fungal burden in the lungs, without difference in the numbers of PMN in any compartment (blood, BALF, lung tissue) was thereby most likely facilitated by the existence of NET formation. Interestingly, *Pad4*$^{-/-}$ mice displayed significantly less acute lung injury compared to wildtype mice, which was assessed by measuring albumin concentration in the BALF as a surrogate marker for the disruption of alveolar-capillary barrier integrity (Fig. 2B).

Next, we hypothesized whether the differences in fungal clearance affect the release of inflammatory mediators in the lungs. The *Pad4*$^{-/-}$ mice showed a lower amount of TNF-α in the BALF compared to the wildtype mice, whereas the control animals had no detectable quantities of TNFα (Fig. 2C). However, the difference between *Pad4*$^{-/-}$ and wildtype mice was not statistically significant. Furthermore, *Pad4*$^{-/-}$ and wildtype mice exhibited a differential cytokine profile during IPA. While the amounts of cytokines such as GM-CSF, IL-1β, IL-10 and IL-6 were lower in *Pad4*$^{-/-}$ compared to the wildtype mice (Fig. 2D–G), MCP-1 and M-CSF were elevated in *Pad4*$^{-/-}$ animals (Fig. 2H–I). Overall, 22 cytokines where analyzed by a bead-based immunoassay, some showing only minor differences. Furthermore, trends for higher amounts in wildtype mice were observed for G-CSF, GRO-α, IFN-γ, IL-12p70, IL-17A, IL-23, IP-10, MIP-1α, MIP-2, RANTES and TNFα. Similar cytokine amounts where observed for Eotaxin, IL-18, IL-7 and MIP-1β in the two mice strains. MCP-3 was present in higher concentration in *Pad4*$^{-/-}$ mice (data not shown).

3.3. Other PMN functions of Pad4$^{-/-}$ mice are not altered in vitro

NET formation has been described to be an important effector function of PMN, nevertheless defective NET formation in *Pad4*$^{-/-}$ mice resulted in improved fungal clearance during IPA and in reduced acute lung injury in this study (Figs. 1 and 2). Therefore, we were interested if other PMN functions, especially those contributing to fungal killing are more pronounced in compensating PAD4 deficiency.

White blood cells (WBC) from lysed blood of *Pad4*$^{-/-}$ and wildtype mice were activated with indicated stimuli and PMN functions were analyzed by flow cytometry. Whereas enhanced phagocytosis of PE-labeled *A. fumigatus* conidia was detectable after incubation at 37 °C for 2 h compared to control samples at 4 °C, phagocytosis did not vary between wildtype and *Pad4*$^{-/-}$ mice (Fig. 3A). Furthermore, WBC were incubated with fungal stimuli, zymosan and *A. fumigatus* conidia, and with the bacterial compound lipopolysaccharides (LPS). After 2 h WBC were analyzed for oxidative burst, degranulation – enhanced CD11b surface expression – and CD62 L shedding representing PMN effector functions. While these different compounds lead to WBC activation, no significant differences were observed between WBC from wildtype and *Pad4*$^{-/-}$ mice (Fig. 3B–D). PMN functions where also analyzed in purified murine PMN enriched from bone marrow. Again, no differences were observed after activation with mentioned stimuli in PMN from wildtype and *Pad4*$^{-/-}$ mice (data not shown).

3.4. Human PMN functions are not altered after PAD4 inhibition

To evaluate the effects of PAD4 deficiency in a human setting, PMN functions from healthy human donors were analyzed after the incubation with a PAD4 inhibitor. PMN were preincubated for 30 min with a PAD4 inhibitor (GSK 484, 10 μM) and phagocytosis of PE-labeled *A. fumigatus* conidia was analyzed after 1 h. Whereas enhanced phagocytosis of PE-labeled *A. fumigatus* conidia was detectable after incubation at 37 °C compared to control samples at 4 °C, we did not detect any differences in phagocytic activity between inhibitor-treated and control cells (Fig. 4A). Human PMN were furthermore activated with zymosan, *A. fumigatus* conidia and LPS. Degranulation and shedding were analyzed by flow cytometry, detecting activation of PMN, but again we did not discover any significant differences in CD11b and CD62 L surface expression between PAD4 inhibitor-treated and control cells (Fig. 4B–C). Oxidative burst from PMN was analyzed after activation with the same fungal and bacterial substances and with or without PAD4 inhibitor pretreatment. Zymosan, *A. fumigatus* conidia and LPS induced the activation of PMN, but this was independent of pretreatment with the inhibitor (Fig. 4D). Since an extension of the short life span of PMN is also essential for their antimicrobial activity, their viability after activation with the above mentioned stimuli was assessed. As expected, the activation of PMN prolonged their viability, but the inhibition of PAD4 did not affect this PMN function (Fig. 4E). Therefore, PAD4 inhibition in human PMN does not result in differential regulation of PMN functions other than NET formation *in vitro*.

3.5. NET formation does not result in permanent lung damage after IPA

Since PAD4 deficiency in mice improved the course of IPA after 24 h, we hypothesized if the superior course of this infectious disease in *Pad4*$^{-/-}$ mice results in better longterm

outcome regarding lung function one week after IPA. Invasive lung function analysis was therefore performed one week after the induction of IPA by challenging infected or control mice *i.t.* with increasing doses of methacholine. Besides increased airway resistance (RI) along with escalating concentrations of methacholine in all mice, the lung function test did not detect any significant differences in airway resistance in wildtype and *Pad4*$^{-/-}$ animals (Fig. 5A). Furthermore, BALF was analyzed. The amount of WBC had dramatically decreased one week after infection (Fig. 5B) compared to results after one day (Fig. 2A), therefore the fraction of PMN was not detectable anymore. The amounts of albumin in BALF appeared somewhat lower after one weeks as compared to 24 h. No differences in albumin were observed between wildtype and *Pad4*$^{-/-}$ mice at this late phase of IPA (Fig. 5C). Similar as after 24 h of IPA, pulmonary inflammation did not vary between wildtype and *Pad4*$^{-/-}$ mice after one week of IPA (Fig. 5D). We also compared the inflammatory response after one day and one week of IPA. After one week the previously higher amounts of IL-27 in wildtype compared to *Pad4*$^{-/-}$ mice were not detectable anymore (data not shown).

4. Discussion/Conclusion

In this study, we demonstrate that the presence of PAD4, which has been described as major player for the formation of NETosis plus neutrophil cytoplasts (Krishnamoorthy et al., 2018), impairs fungal clearance in a mouse model of IPA and contributes to acute lunge injury, assessed by albumin load in the BALF (Matute-Bello et al., 2011) 24 h after infection. NETs are composed of DNA, histones and granular proteins such as NE and MPO. In direct interaction with epithelial and endothelial cells it has been shown that histones and MPO are responsible for NET-mediated cytotoxicity (Saffarzadeh et al., 2012). Hence, NETs contribute to a vicious cycle of lung injury and inflammation. They are considered to be degraded by DNase enzymes and macrophages, that internalize and remove DNA, as well as other cellular debris. A balance between NETosis and NET clearance is therefore essential for effectively clearing infectious agents with minimal damage to the lungs (Cheng and Palaniyar, 2013) that seems to be disrupted in PAD4 deficiency. During infection and inflammation in the lungs, various cells (e.g. endothelial, epithelial, immune cells) express inflammatory cytokines, chemokines, and growth factors to recruit monocytes (e.g., MCP-1) and PMN (e.g., IL-8, or KC/MIP-2 as murine homologous, respectively) into the airway lumen (Cheng and Palaniyar, 2013). Therefore the improved course of IPA in PAD4 deficiency, which is accompanied by a differential cytokine profile, might be due to a more pronounced monocytic inflammatory response in *Pad4*$^{-/-}$ mice, compared to wildtype mice (Fig. 2C–I), since these immune cells also play an important role in innate antifungal immunity in the lung and are capable of direct fungal spore elimination (Espinosa et al., 2014). Furthermore reduced levels of IL-17A in PAD4 deficiency might be due to the existence of cytoplasts, since enucleated neutrophil cytoplasts activate lung dendritic cells and trigger antigen-specific IL-17A production from naïve CD4^{+} T cells (Krishnamoorthy et al., 2018). Interestingly, the differences in the course of infection did not result in permanent lung damage as analyzed by lung function test and overall was not apparent any more one week after infection (Fig. 5). Previous studies showed that wildtype mice suffer from clinical signs of pneumonia, but all animals survive the infection and the development of *A.*

fumigatus conidia to hyphae nearly fails to appear (Alflen et al., 2017; Stadler et al., 2017). Since PMN sense microbe size and selectively release NETs in response to large pathogens like *A. fumigatus* hyphae or large aggregated conidia but not in response to small single conidia (Branzk et al., 2014), the presence of NET formation may play only a minor role in healthy individuals like wildtype mice. The less effective course of IPA in wildtype compared to *Pad4*$^{-/-}$ mice seems to be rather a retarded clearance of fungal compounds because the differences are absent after one week. Nevertheless, some NET formation takes place in the wildtype mice suffering from IPA, since citH3 is detectable and is the most likely contribution to the pronounced acute lung injury in wildtype compared to *Pad4*$^{-/-}$ mice.

Several studies showed, that PAD4 is dispensable in different diseases and contributes to organ damage. Though PAD4 is required for NET formation in response to *A. fumigatus*, PAD4-dependent NETosis is not required for *A. fumigatus* killing either *in vitro* or during infection (Clark et al., 2018), and PAD2/PAD4 inhibition alleviates LPS-induced pulmonary dysfunction by preventing vascular leakage and improves survival in a mouse model of lethal endotoxemia. *In vitro* it was demonstrated, that LPS-activated PMN produce citH3 and derived NETs increase the permeability of endothelial cells (Liang et al., 2018). Apart from that, the pathogenicity of NET is especially important in pulmonary diseases due to the lung architecture itself, in which cases tissue damage and impairment in lung function is enhanced (Porto and Stein, 2016). NETosis furthermore contributes to age-related organ damage since PAD4 promotes organ fibrosis and dysfunction (Martinod et al., 2017). Therefore, especially patients with an existing lung damage like cystic fibrosis, asthma and chronic obstructive pulmonary disease (COPD) (Porto and Stein, 2016) might be at risk of an irreversible and severe lung damage after additionally experiencing IPA and therefore benefit from a therapy that targets and inhibits NET formation to prevent further lung injury.

The differential course of infection in *Pad4*$^{-/-}$ and wildtype mice was not caused by altered PMN recruitment, and PMN functions other than NET formation were not compensatory increased, whether in murine PMN of *Pad4*$^{-/-}$ and wildtype mice *ex vivo*, nor in isolated human PMN after PAD4 inhibition. Unfortunately, obtaining sufficient numbers of purified murine PMN is only possible with bone marrow derived PMN. However, functions of peripheral blood and bone marrow PMN might be different. Furthermore, it should be noted, that the exact mechanisms of fungal killing in mice can actually be different from those observed in humans, since human PMN have distinct killing mechanisms for *Candida* and *Aspergillus* for both their conidia and their hyphae (Gazendam et al., 2016).

Another limitation of our study is, that NET formation was exclusively assessed by measuring citH3, which may not totally reflect NETosis since several signaling mechanisms have been identified to induce this PMN function (Kenny et al., 2017). Although studies in mice strongly suggest, that PAD4 deficiency leads to decreased citH3 and inability of PMN to form NETs (Martinod et al., 2013), our conclusion is based on these data, without any other testing of NET formation.

In conclusion, our study highlights the negative contribution of NET release in fungal infection in a vulnerable organ such as the lung. Inhibition of NET formation might

therefore be a useful strategy to avoid lung damage in immunocompromised patients, especially in those suffering from preexisting pulmonary disease.

Acknowledgements

We thank Petra Schuster for excellent technical assistance and Sabine Reyda for providing *Pad4*$^{-/-}$ mice.

Funding sources

This work was supported by the Federal Ministry of Education and Research Grant 01EO1503, the Deutsche Forschungsgemeinschaft (BO3482/3-3, BO3482/4-1, to M.B.) and by the National Institutes of Health (1R01HL141513, 1R01HL139641, to M.B.). The funding organizations had no role in study design, data collection and analysis, decision to publish, or preparation of the manuscript.

Statement of ethics

All animal experiments conform to internationally accepted standards. All procedures were performed in accordance with the institutional guidelines and approved by the responsible national authority (National Investigation Office Rheinland-Pfalz, Approval ID: AZ 23 177-07/G16-1-020E1).

Human studies were performed after obtaining written informed consent from healthy volunteer donors and were approved by the local ethics committee according to the institutional guidelines (Landesärztekammer Rheinland-Pfalz, Approval no. 837.258.17 (11092)).

References

Alflen A, Prüfer S, Ebner K, Reuter S, Aranda Lopez P, Scharrer I, Banno F, Stassen M, Schild H, Jurk K, Bosmann M, Beckert H, Radsak MP, 2017 ADAMTS-13 regulates neutrophil recruitment in a mouse model of invasive pulmonary aspergillosis. Sci. Rep 7, 7184 10.1038/s41598-017-07340-3. [PubMed: 28775254]

Alflen A, Stadler N, Aranda Lopez P, Teschner D, Theobald M, Heß G, Radsak MP, 2018 Idelalisib impairs TREM-1 mediated neutrophil inflammatory responses. Sci. Rep 8, 5558 10.1038/s41598-018-23808-2. [PubMed: 29615799]

Bosmann M, Russkamp NF, Strobl B, Roewe J, Balouzian L, Pache F, Radsak MP, van Rooijen N, Zetoune FS, Sarma JV, Núñez G, Müller M, Murray PJ, Ward PA, 2014 Interruption of macrophage-derived IL-27(p28) production by IL-10 during sepsis requires STAT3 but not SOCS3. J. Immunol 193, 5668–5677. 10.4049/jimmunol.1302280. [PubMed: 25348624]

Böhm L, Maxeiner J, Meyer-Martin H, Reuter S, Finotto S, Klein M, Schild H, Schmitt E, Bopp T, Taube C, 2015 IL-10 and regulatory T cells cooperate in allergen-specific immunotherapy to ameliorate allergic asthma. J. Immunol 194, 887–897. 10.4049/jimmunol.1401612. [PubMed: 25527785]

Branzk N, Lubojemska A, Hardison SE, Wang Q, Gutierrez MG, Brown GD, Papayannopoulos V, 2014 Neutrophils sense microbe size and selectively release neutrophil extracellular traps in response to large pathogens. Nat. Immunol 15, 1017–1025. 10.1038/ni.2987. [PubMed: 25217981]

Brinkmann V, Reichard U, Goosmann C, Fauler B, Uhlemann Y, Weiss DS, Weinrauch Y, Zychlinsky A, 2004 Neutrophil extracellular traps kill bacteria. Science 303, 1532–1535. 10.1126/science.1092385. [PubMed: 15001782]

Chamilos G, Luna M, Lewis RE, Bodey GP, Chemaly R, Tarrand JJ, Safdar A, Raad II, Kontoyiannis DP, 2006 Invasive fungal infections in patients with hematologic malignancies in a tertiary care cancer center: an autopsy study over a 15-year period (1989–2003). Haematologica 91, 986–989. [PubMed: 16757415]

Cheng OZ, Palaniyar N, 2013 NET balancing: a problem in inflammatory lung diseases. Front. Immunol 4, 1 10.3389/fimmu.2013.00001. [PubMed: 23355837]

Clark HL, Abbondante S, Minns MS, Greenberg EN, Sun Y, Pearlman E, 2018 Protein deiminase 4 and CR3 regulate Aspergillus fumigatus and β-Glucan-Induced neutrophil extracellular trap formation, but hyphal killing is dependent only on CR3. Front. Immunol 9, 1532 10.3389/fimmu.2018.01182. [PubMed: 30038613]

Demla A, Madsen LT, Dains J, 2016 Effectiveness of granulocyte transfusions in neutropenic adult oncology patients: a comprehensive review of the literature. J. Adv. Pract. Oncol 7, 410–417. [PubMed: 29225999]

Espinosa V, Jhingran A, Dutta O, Kasahara S, Donnelly R, Du P, Rosenfeld J, Leiner I, Chen C-C, Ron Y, Hohl TM, Rivera A, 2014 Inflammatory monocytes orchestrate innate antifungal immunity in the lung. PLoS Pathog. 10, e1003940 10.1371/journal.ppat.1003940.

Gazendam RP, van de Geer A, Roos D, van den Berg TK, Kuijpers TW, 2016 How neutrophils kill fungi. Immunol. Rev 273, 299–311. 10.1111/imr.12454. [PubMed: 27558342]

Haselmayer P, Grosse-Hovest L, von Landenberg P, Schild H, Radsak MP, 2007 TREM-1 ligand expression on platelets enhances neutrophil activation. Blood 110, 1029–1035. 10.1182/blood-2007-01-069195. [PubMed: 17452516]

Hemmers S, Teijaro JR, Arandjelovic S, Mowen KA, 2011 PAD4-mediated neutrophil extracellular trap formation is not required for immunity against influenza infection. PLoS One 6, e22043 10.1371/journal.pone.0022043.

Kapp K, Prüfer S, Michel CS, Habermeier A, Luckner-Minden C, Giese T, Bomalaski J, Langhans C-D, Kropf P, Müller I, Closs EI, Radsak MP, Munder M, 2014 Granulocyte functions are independent of arginine availability. J. Leukoc. Biol 96, 1047–1053. 10.1189/jlb.3AB0214-082R. [PubMed: 25104794]

Kenny EF, Herzig A, Krüger R, Muth A, Mondal S, Thompson PR, Brinkmann V, Bernuth HV, Zychlinsky A, 2017 Diverse stimuli engage different neutrophil extracellular trap pathways. Elife 6, 178 10.7554/eLife.24437.

Kolaczkowska E, Kubes P, 2013 Neutrophil recruitment and function in health and inflammation. Nat. Rev. Immunol 13, 159–175. 10.1038/nri3399. [PubMed: 23435331]

Kontoyiannis DP, Marr KA, Park BJ, Alexander BD, Anaissie EJ, Walsh TJ, Ito J, Andes DR, Baddley JW, Brown JM, Brumble LM, Freifeld AG, Hadley S, Herwaldt LA, Kauffman CA, Knapp K, Lyon GM, Morrison VA, Papanicolaou G, Patterson TF, Perl TM, Schuster MG, Walker R, Wannemuehler KA, Wingard JR, Chiller TM, Pappas PG, 2010 Prospective surveillance for invasive fungal infections in hematopoietic stem cell transplant recipients, 2001–2006: over-view of the Transplant-Associated Infection Surveillance Network (TRANSNET) Database. Clin. Infect. Dis 50, 1091–1100. 10.1086/651263. [PubMed: 20218877]

Krishnamoorthy N, Douda DN, Brüggemann TR, Ricklefs I, Duvall MG, Abdulnour R-EE, Martinod K, Tavares L, Wang X, Cernadas M, Israel E, Mauger DT, Bleecker ER, Castro M, Erzurum SC, Gaston BM, Jarjour NN, Wenzel S, Dunican E, Fahy JV, Irimia D, Wagner DD, Levy BD, National Heart, Lung, and Blood Institute Severe Asthma Research Program-3 Investigators, 2018 Neutrophil cytoplasts induce TH17 differentiation and skew inflammation toward neutrophilia in severe asthma. Sci. Immunol 3, eaao4747 10.1126/sciimmunol.aao4747.

Lewis HD, Liddle J, Coote JE, Atkinson SJ, Barker MD, Bax BD, Bicker KL, Bingham RP, Campbell M, Chen YH, Chung C-W, Craggs PD, Davis RP, Eberhard D, Joberty G, Lind KE, Locke K, Maller C, Martinod K, Patten C, Polyakova O, Rise CE, Rüdiger M, Sheppard RJ, Slade DJ, Thomas P, Thorpe J, Yao G, Drewes G, Wagner DD, Thompson PR, Prinjha RK, Wilson DM, 2015 Inhibition of PAD4 activity is sufficient to disrupt mouse and human NET formation. Nat. Chem. Biol 11, 189–191. 10.1038/nchembio.1735. [PubMed: 25622091]

Liang Y, Pan B, Alam HB, Deng Q, Wang Y, Chen E, Liu B, Tian Y, Williams A, Duan X, Wang Y, Zhang J, Li Y, 2018 Inhibition of peptidylarginine deiminase alleviates LPS-induced pulmonary dysfunction and improves survival in a mouse model of lethal endotoxemia. Eur. J. Pharmacol 833, 432–440. 10.1016/j.ejphar.2018.07.005. [PubMed: 29981294]

Margalit A, Kavanagh K, 2015 The innate immune response to Aspergillus fumigatus at the alveolar surface. FEMS Microbiol. Rev 39, 670–687. 10.1093/femsre/fuv018. [PubMed: 25934117]

Martinod K, Demers M, Fuchs TA, Wong SL, Brill A, Gallant M, Hu J, Wang Y, Wagner DD, 2013 Neutrophil histone modification by peptidylarginine deiminase 4 is critical for deep vein thrombosis in mice. Proc. Natl. Acad. Sci. U. S. A 110, 8674–8679. 10.1073/pnas.1301059110. [PubMed: 23650392]

Martinod K, Witsch T, Erpenbeck L, Savchenko A, Hayashi H, Cherpokova D, Gallant M, Mauler M, Cifuni SM, Wagner DD, 2017 Peptidylarginine deiminase 4 promotes age-related organ fibrosis. J. Exp. Med 214, 439–458. 10.1084/jem.20160530. [PubMed: 28031479]

Matute-Bello G, Downey G, Moore BB, Groshong SD, Matthay MA, Slutsky AS, Kuebler WM, Acute Lung Injury in Animals Study Group, 2011 An official American Thoracic Society workshop report: features and measurements of experimental acute lung injury in animals. Presented at the American Journal of Respiratory Cell and Molecular Biology, American Thoracic Society 725–738. 10.1165/rcmb.2009-0210ST.

Metzler KD, Goosmann C, Lubojemska A, Zychlinsky A, Papayannopoulos V, 2014 A myeloperoxidase-containing complex regulates neutrophil elastase release and actin dynamics during NETosis. Cell Rep. 8, 883–896. 10.1016/j.celrep.2014.06.044. [PubMed: 25066128]

Pagano L, Caira M, Candoni A, Offidani M, Martino B, Specchia G, Pastore D, Stanzani M, Cattaneo C, Fanci R, Caramatti C, Rossini F, Luppi M, Potenza L, Ferrara F, Mitra ME, Fadda RM, Invernizzi R, Aloisi T, Picardi M, Bonini A, Vacca A, Chierichini A, Melillo L, de Waure C, Fianchi L, Riva M, Leone G, Aversa F, Nosari A, 2010 Invasive aspergillosis in patients with acute myeloid leukemia: a SEIFEM-2008 registry study. Haematologica 95, 644–650. 10.3324/haematol.2009.012054. [PubMed: 19850903]

Pappas PG, Alexander BD, Andes DR, Hadley S, Kauffman CA, Freifeld A, Anaissie EJ, Brumble LM, Herwaldt L, Ito J, Kontoyiannis DP, Lyon GM, Marr KA, Morrison VA, Park BJ, Patterson TF, Perl TM, Oster RA, Schuster MG, Walker R, Walsh TJ, Wannemuehler KA, Chiller TM, 2010 Invasive fungal infections among organ transplant recipients: results of the Transplant-Associated Infection Surveillance Network (TRANSNET). Clin. Infect. Dis 50, 1101–1111. 10.1086/651262. [PubMed: 20218876]

Porto BN, Stein RT, 2016 Neutrophil extracellular traps in pulmonary diseases: too much of a good thing? Front. Immunol 7, 311 10.3389/fimmu.2016.00311. [PubMed: 27574522]

Prüfer S, Weber M, Stein P, Bosmann M, Stassen M, Kreft A, Schild H, Radsak MP, 2014 Oxidative burst and neutrophil elastase contribute to clearance of Aspergillus fumigatus pneumonia in mice. Immunobiology 219, 87–96. 10.1016/j.imbio.2013.08.010. [PubMed: 24054721]

Reuter S, Martin H, Beckert H, Bros M, Montermann E, Belz C, Heinz A, Ohngemach S, Sahin U, Stassen M, Buhl R, Eshkind L, Taube C, 2014 The Wnt/β-catenin pathway attenuates experimental allergic airway disease. J. Immunol 193, 485–495. 10.4049/jimmunol.1400013. [PubMed: 24929002]

Romani L, 2004 Immunity to fungal infections. Nat. Rev. Immunol 4, 1–23. 10.1038/nri1255. [PubMed: 14661066]

Saffarzadeh M, Juenemann C, Queisser MA, Lochnit G, Barreto G, Galuska SP, Lohmeyer J, Preissner KT, 2012 Neutrophil extracellular traps directly induce epithelial and endothelial cell death: a predominant role of histones. PLoS One 7, e32366 10.1371/journal.pone.0032366.

Stadler N, Hasibeder A, Aranda Lopez P, Teschner D, Desuki A, Kriege O, Weber ANR, Schulz C, Michel C, Heß G, Radsak MP, 2017 The Bruton tyrosine kinase inhibitor ibrutinib abrogates triggering receptor on myeloid cells 1 mediated neutrophil activation. Haematol. Haematol. 10.3324/haematol.2016.152017.2016.152017.

Stewart ER, Thompson GR, 2016 Treatment of primary pulmonary aspergillosis: an assessment of the evidence. J. Fungi (Basel) 2, 25 10.3390/jof2030025.

Urban CF, Reichard U, Brinkmann V, Zychlinsky A, 2006 Neutrophil extracellular traps capture and kill Candida albicans yeast and hyphal forms. Cell. Microbiol 8, 668–676. 10.1111/j.1462-5822.2005.00659.x. [PubMed: 16548892]

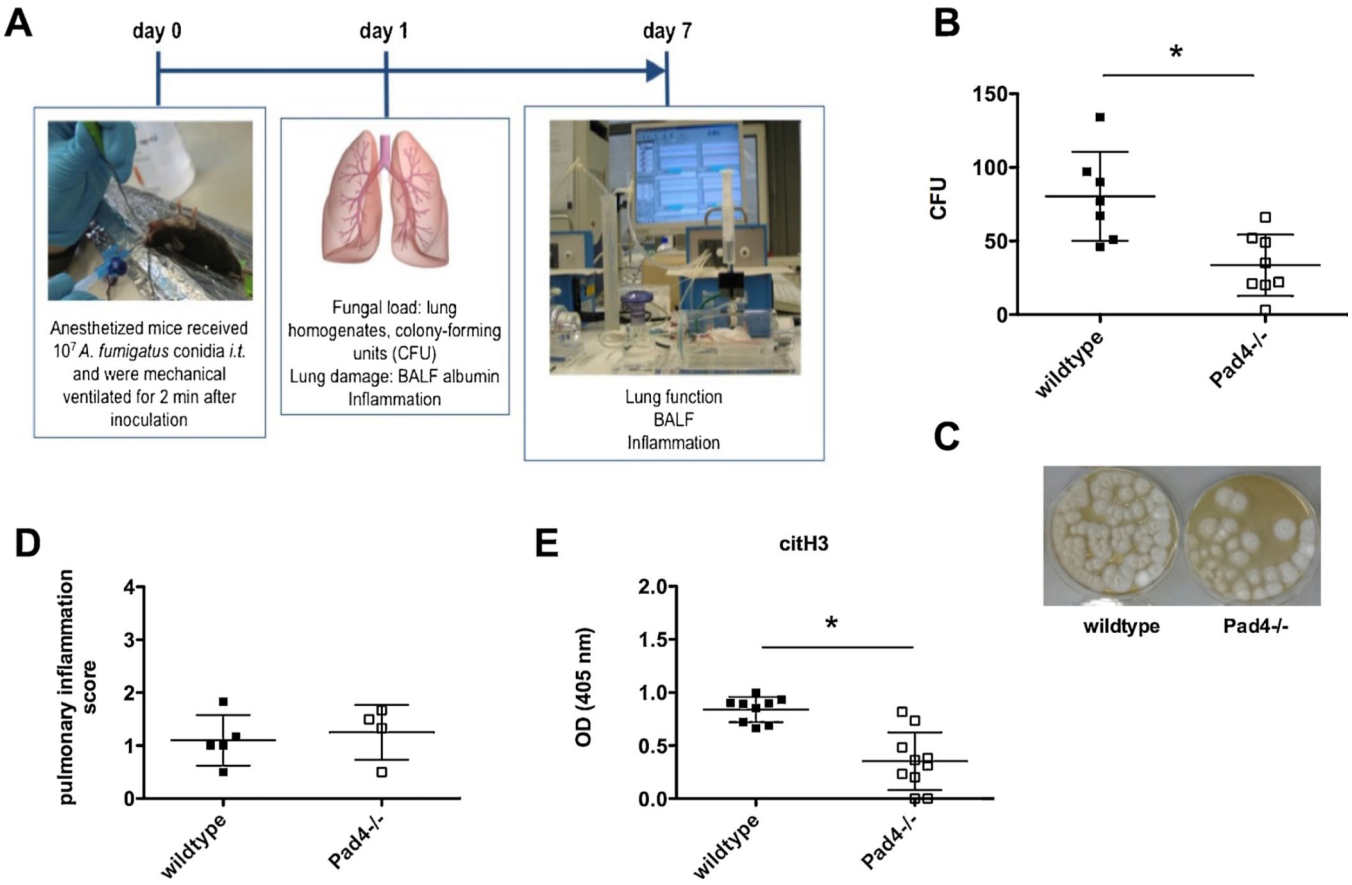

Fig. 1.

PAD4 deficiency improves fungal clearance 24 h after IPA. (A) To study IPA in a murine model, mice were infected *i.t.* with 10^7 *A. fumigatus* conidia and were mechanically ventilated for 2 min. Severity and course of infection was analyzed after 24 h by different read outs, as well as after one week by additionally performing invasive lung function tests. (B) 24 h after infection fungal burden in the lungs was analyzed in *Pad4*$^{-/-}$ and wildtype mice, after homogenizing lungs, plating and culturing them on agar for 24 h. Fungal burden was assessed as colony forming units (CFU). Depicted are the cumulative results (mean plus SD) of two independent experiments (wildtype n = 7, *Pad4*$^{-/-}$ n = 8). (C) Representative CFU samples after culturing them for 48 h from wildtype and *Pad4*$^{-/-}$ mice are depicted. (D) Pulmonary inflammation was evaluated in a blinded fashion by H.B. on H&E stained lung tissue sections 24 h after IPA. Depicted are the results (mean plus SD) of one independent experiment out of two (wildtype n = 5, *Pad4*$^{-/-}$ n = 4). (E) 24 h after IPA BALF was analyzed for citH3 by an ELISA at an optical density (OD) of 405 nm. Depicted are the cumulative results (mean plus SD) of two experiments (wildtype n = 9, *Pad4*$^{-/-}$ n = 10). (*) indicates a significant difference ($p < 0.05$) by Mann-Whitney *U* test.

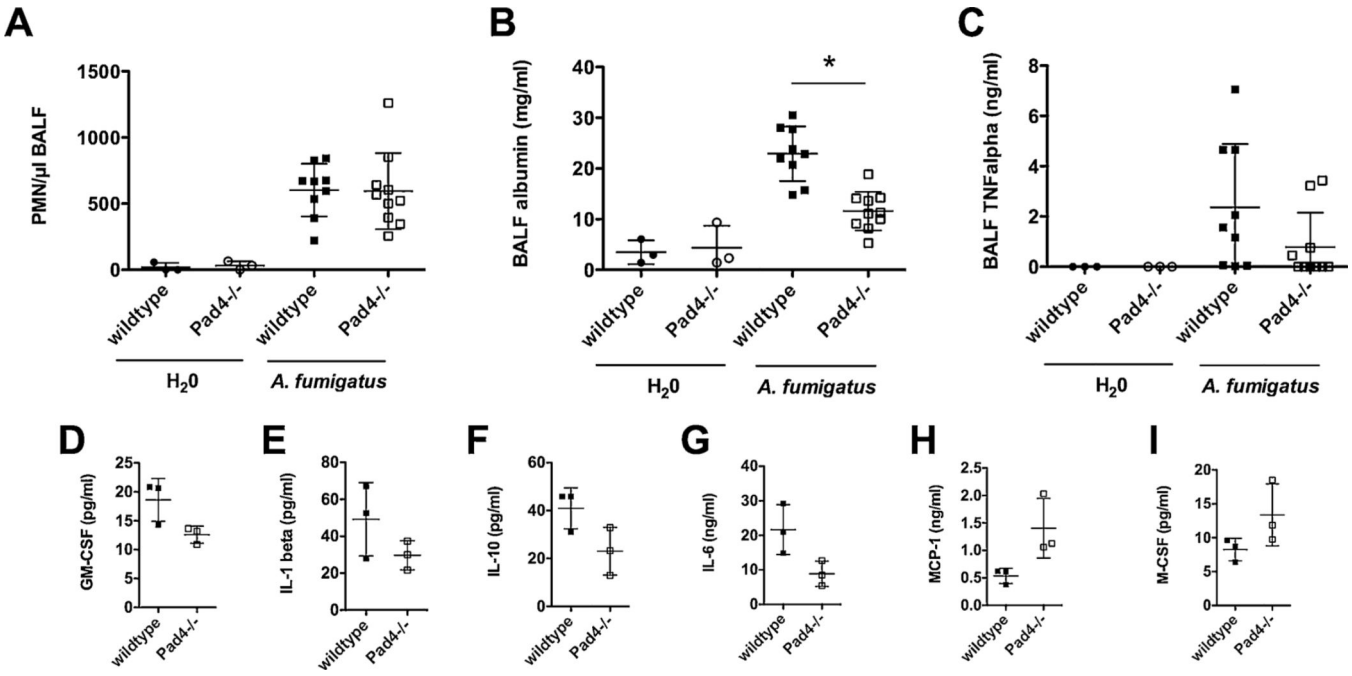

Fig. 2.

PAD4 deficiency reduces lung damage 24 h after IPA. 24 h after the induction of IPA, *Pad4*$^{-/-}$ and wildtype mice were analyzed. (A) PMN recruitment to the BALF, (B) BALF albumin and (C) TNFα amount was assessed. Depicted are the cumulative results (mean plus SD) of one (H_2O-treated wildtype n = 3, *Pad4*$^{-/-}$ n = 3) or two independent experiments (*A. fumigatus*-treated wildtype n = 9, *Pad4*$^{-/-}$ n = 10). (*) indicates a significant difference ($p < 0.05$) by one-way ANOVA with Bonferroni's posttest. (D–I) BALF samples were pooled (each a total of 3 samples from wildtype n = 9 and *Pad4*$^{-/-}$ n = 10 out of 2 independent experiments) and inflammation was analyzed by a customized 22-plex ProcartaPlex and measured with BioPlex 200. Depicted are mean plus SD.

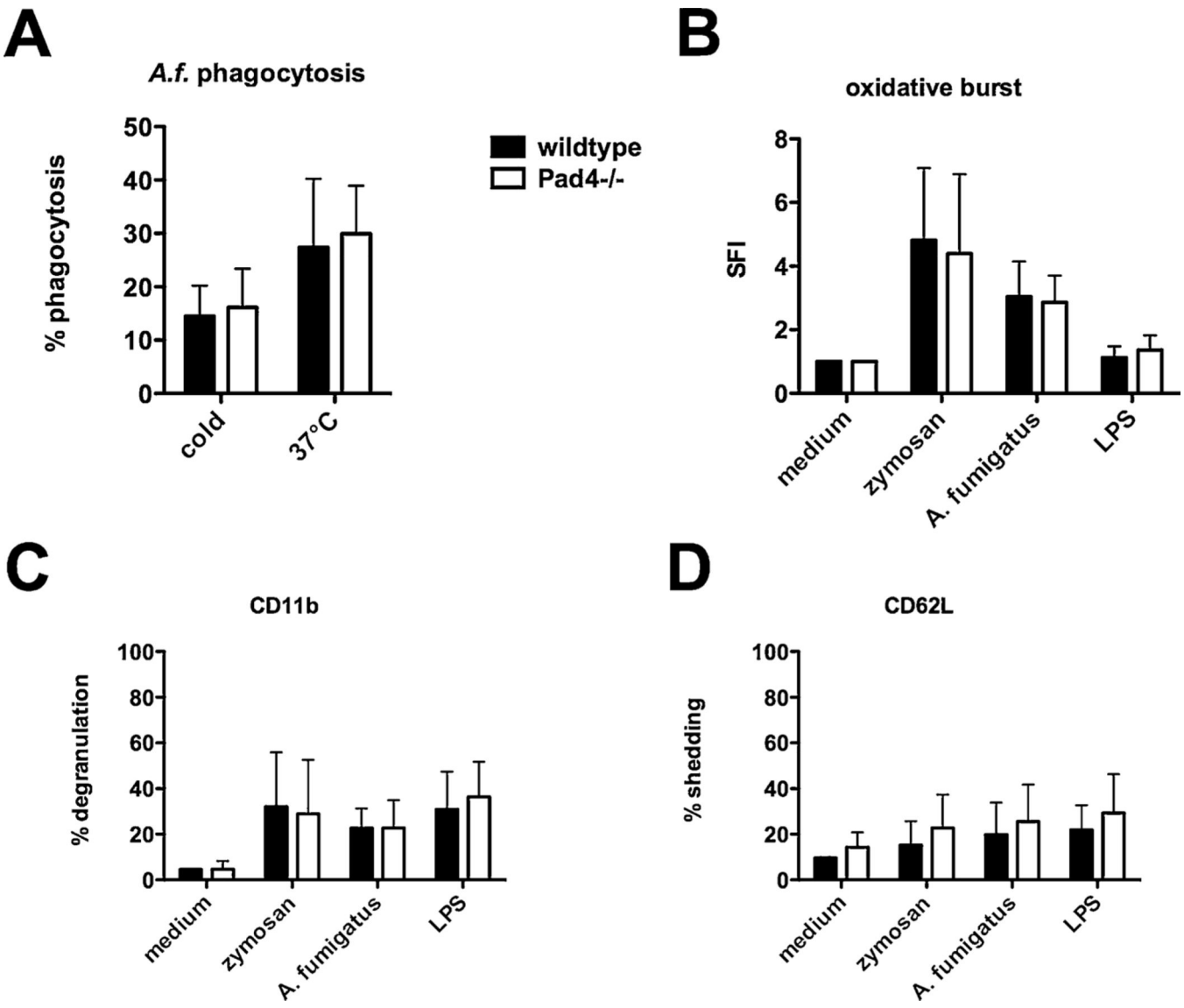

Fig. 3.

Other PMN functions of *Pad4*$^{-/-}$ mice are not altered *in vitro*. WBC were isolated from blood of *Pad4*$^{-/-}$ and wildtype mice. For phagocytosis of fungal compounds cells were incubated with PE-labeled *A. fumigatus* conidia at 37 °C for 2 h, samples incubated at 4 °C served as negative control. (B) Oxidative burst activity was assessed as SFI after activating cells with respective stimulus, as well as (C) degranulation (CD11b surface expression) and (D) CD62 L shedding. Cumulative results (mean plus SD) of five independent experiments are depicted. A two-way ANOVA with Bonferroni's posttest detects no significant difference ($p < 0.05$) between WBC from wildtype and *Pad4*$^{-/-}$ mice.

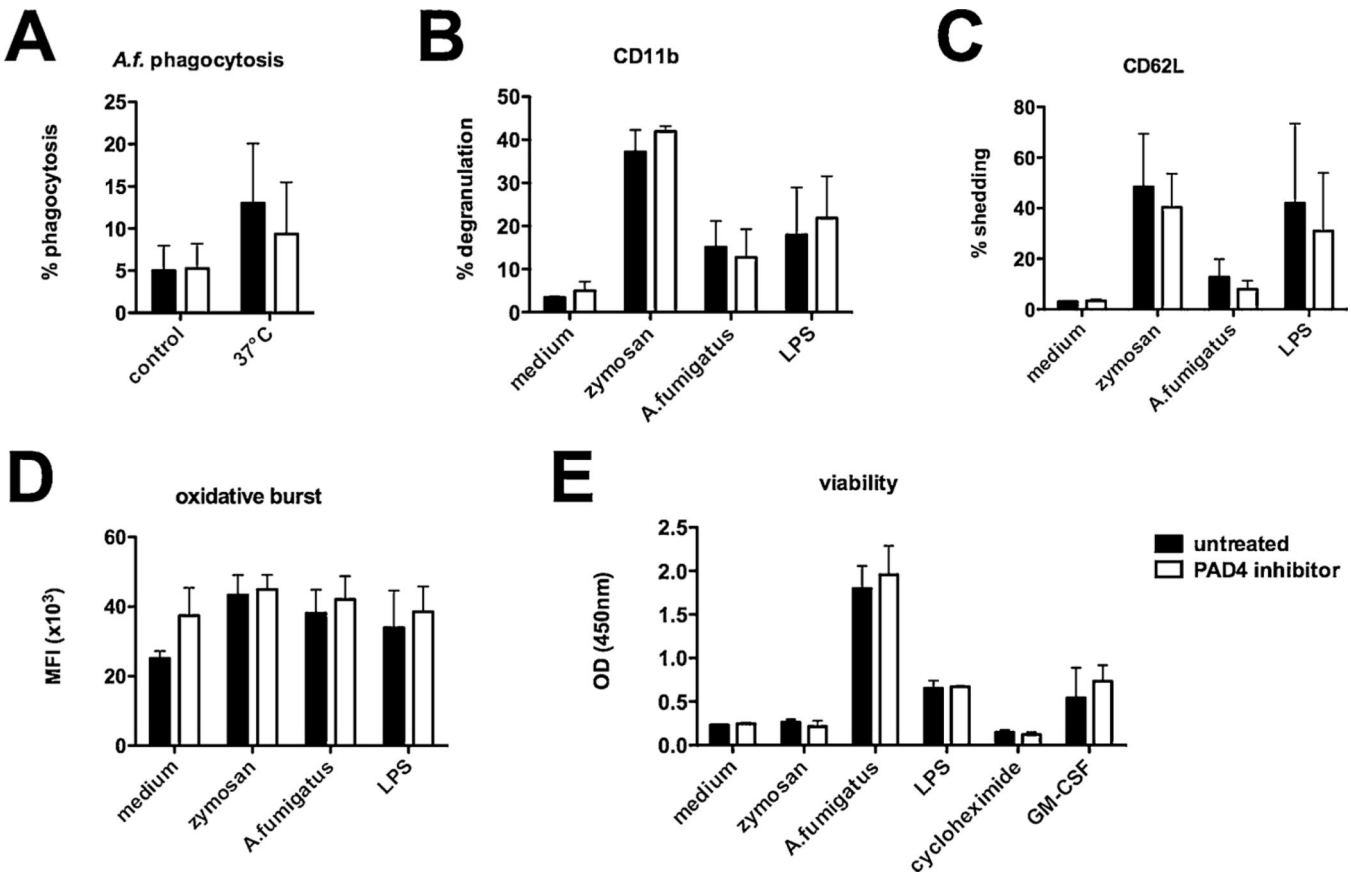

Fig. 4.

Human PMN functions are not altered after PAD4 inhibition. Human PMN from healthy donors were isolated and activated as indicated. Some cells were preincubated for 30 min with a PAD4 inhibitor. (A) For phagocytosis of fungal compounds cells were incubated with PE-labeled *A. fumigatus* conidia at 37 °C for 1 h, samples incubated at 4 °C served as negative control. (B) degranulation (CD11b surface expression) and (C) CD62 L shedding were assessed by flow cytometry after 1 h. (D) Oxidative burst activity was analyzed as fluorescence kinetics and results after 2 h are depicted. (E) Viability was measured using a cell proliferation assay, and employing GM-CSF as viability control and cycloheximide treated samples represented dead cells. Cumulative results (mean plus SD) of three independent experiments are depicted. A two-way ANOVA with Bonferroni's posttest detects no significant difference ($p < 0.05$) between PAD4 inhibitor treated and untreated PMN.

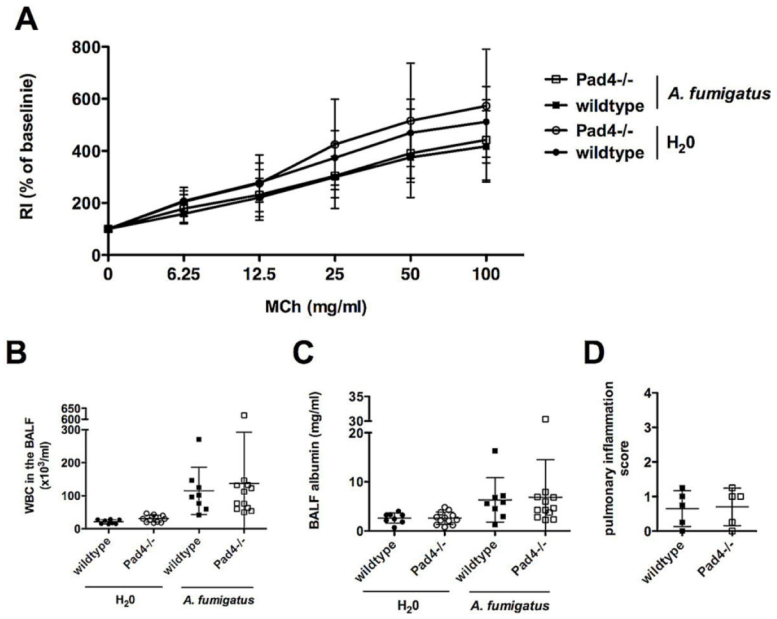

Fig. 5.

NET formation does not result in permanent lung damage after clearance of IPA. Some *Pad4*$^{-/-}$ and wildtype mice were analyzed one week after the induction of IPA. (A) Invasive lung function tests were performed after administering serially increasing doses of methacholine (MCh), and airway hyperresponsiveness was measured as airway resistance (RI). (B) Recruitment of WBC into the airways and (C) albumin amount in the BALF were assessed. (D) Pulmonary inflammation was evaluated in a blinded fashion by H.B. on H&E stained lung tissue sections (5 randomly chosen samples per wildtype and *Pad4*$^{-/-}$) one week after IPA. Depicted are the cumulative results (mean plus SD) of two independent experiments (H_2O-treated wildtype n = 8 and *Pad4*$^{-/-}$ n = 12, *A. fumigatus*-treated wildtype n = 8 and *Pad4*$^{-/-}$ n = 12).